J MATER RES TECHNOL. 2017;xxx(xx):xxx–xxx

Available online at www.sciencedirect.com

jmr&t Journal of Materials Research and Technology

www.jmrt.com.br

Original Article

Corrosion behaviour of S43035 ferritic stainless steel in hot sulphate/chloride solution

Roland Tolulope Loto[a,*], Cleophas Akintoye Loto[a,b]

[a] Department of Mechanical Engineering, Covenant University, Ota, Ogun State, Nigeria

[b] Department of Chemical, Metallurgical and Materials Engineering, Tshwane University of Technology, Pretoria, South Africa

ARTICLE INFO

Article history:
Received 27 April 2017
Accepted 4 July 2017
Available online xxx

Keywords:
Corrosion
Ferritic
Sulfuric
Steel
NaCl
Passivation

ABSTRACT

The corrosion resistance of S43035 ferritic stainless steel at elevated temperatures of 308 K, 328 K, 348 K and 378 K was studied through potentiodynamic polarization test and optical microscopy analysis in 2 M H_2SO_4 at 0%, 1%, 3.5% and 6% NaCl. Results show that increase in temperature and NaCl generally hinders the formation of the passive film. Changes in corrosion rate from 308 K to 378 K at 0% NaCl was marginal. Metastable pitting was absent until 378 K due to increased electrolytic action of SO_4^{2-} ions. In the presence of chlorides at 308 K metastable pitting is visible delaying the formation of stable passive film. Passivation behaviour was absent at temperatures above 308 K due to polarization similar to carbon steels and a strong decrease in hydrogen evolution over potential especially at 1% and 3.5% NaCl. Optical images showed mild deterioration at 378 K from 0% NaCl and the formation of corrosion pits at 308 K and 378 K from 6% NaCl. Negative enthalpy value at 0% NaCl implies exothermic nature of the steel corrosion reaction. Addition of chlorides changed the steel corrosion reaction to endothermic. Increase in NaCl concentration caused a decrease in activation energy and increase in entropy values due to decrease in passivation of the alloy and consequently increase in corrosion rate. Statistical analysis through ANOVA at confidence levels of 95% and 97.5% showed the strong influence of temperature variation on corrosion rate with *F*-values of 5.256 at 50.8% in contrast to the NaCl concentration whose value was below the significance level.

1. Introduction

Corrosion of stainless steel in reducing/oxidizing environments is a fundamental academic and industrial concern due to the secondary problems associated with it [1]. Stainless steels exhibit exceptional corrosion resistance characteristics in conditions deleterious to carbon steels, and non-ferrous metals and alloys due to the presence of chromium and other alloying elements. The chromium, when in contact with oxygen, forms a barrier of chromium oxide called a

* *Corresponding author.*
E-mail: tolu.loto@gmail.com (R.T. Loto).

http://dx.doi.org/10.1016/j.jmrt.2017.07.004

Please cite this article in press as: Loto RT, Loto CA. Corrosion behaviour of S43035 ferritic stainless steel in hot sulphate/chloride solution. J Mater Res Technol. 2017. http://dx.doi.org/10.1016/j.jmrt.2017.07.004

"passive film" which shields the alloy from aggressive ions. This property enables their extensive application in desalination plants, pharmaceutical industry, thermal power plant, chemical cleaning and pickling process, automobile industry and petrochemical plants due to their stability and strong resistance to redox reactions. However these steels are not impervious to corrosion in specific environments resulting in the initiation and propagation of localized corrosion [2,3]. Localized corrosion occurs in many forms in structures made of these steels during service in various aggressive media such as intergranular and pitting corrosion, sulphide and chloride stress cracking etc. Corrosion due to acids and chlorides are one of the major causes of stainless steel corrosion. In petroleum refining units it represents a significant portion of loss as a result of lost production, inefficient operation, high maintenance and the cost of corrosion control chemicals. During cracking of petroleum, acids appear as a result of hydrolysis of salts which have destructive effect on equipment made of steel [4]. Hydrogen evolution occurs during steel corrosion in acidic solution leading to metal hydrogenation responsible for impairment of their mechanical properties [5].

Numerous investigations have been done to understand the electrochemical characteristics of stainless steels in acidic, chloride and basic mediums, but its corrosion resistance in these media at elevated temperature is limited [6]. The interaction of stainless steels with chemicals and the electrochemical kinetics of their dissolution are basically subject to the formation and collapse of their protective films which has been the subject of in-depth research but not especially at high temperatures [7,8]. The kinetics of the protective film formation depends on the rate constants for the interfacial reactions of the electrolytic species and their movement within the film [9]. Increase in temperature causes thinning of the passive film and accelerated dissolution of the steel alloy, thus limiting the operation of the respective equipment [10,11]. Hot process streams have been known present further challenges for production equipment. 316L stainless steels readily crack at temperatures higher than 334 K with a combination of tensile stress and chlorides. 2205 duplex stainless will resist chloride stress-corrosion cracking in simple salt solutions to temperatures of about 392 K [12]. This research aims to study the electrochemical corrosion behaviour of 43035 ferritic stainless steel in sulphate/chloride condition at temperatures of 308 K, 328 K, 348 K and 378 K.

2. Experimental methods

2.1. Materials preparation

S43035 ferritic stainless steel (43035SS) sourced commercially had a nominal composition as shown in Table 1. The steel electrodes after mounting in epoxy resin according to ASTM G59-97 [13] have an exposed surface area of 1.26 cm^2. The steel specimens after machining were abraded with silicon carbide papers before washing with distilled water and propanone for potentiodynamic polarization test according to ASTM G1-03 [14].

2.2. Test solutions

Recrystallized NaCl obtained from Titan Biotech, India was prepared in volumetric concentrations of 0%, 1%, 3.5% and 6% in 200 mL of 2 M H_2SO_4 solution, prepared from analar grade of H_2SO_4 acid (98%, obtained from Sigma Aldrich, USA) with deionized water

2.3. Potentiodynamic polarization test

Potentiodynamic polarization tests were carried out at 308 K, 328 K, 348 K and 378 K with a three electrode system within a glass cell containing the electrolyte solution and a thermometer, using Digi-Ivy 2311 potentiostat interfaced with a computer. The temperature is thermostatically controlled. Polarization plots were obtained at a scan rate of 0.0015 V/s between potentials of −0.5 V and +1.5 V according to ASTM G102-89(2015) [15]. Corrosion current density (J_{cr}, A/cm^2) and corrosion potential (E_{cr}, V) values were obtained using the Tafel extrapolation method. The corrosion rate (C_R) was calculated from the mathematical relationship;

$$C_R = \frac{0.00327 * J_{cr} * E_{qv}}{D} \quad (1)$$

where E_{qv} is the sample equivalent weight in grams. 0.00327 is a constant for corrosion rate calculation in mm/y [16].

2.4. Optical microscopy characterization

Optical images and surface morphology of 43035SS for 0% and 6% NaCl at 308 K and 378 K were analyzed after potentiodynamic polarization test with Omax trinocular through the aid of ToupCam analytical software.

3. Result and discussion

3.1. Potentiodynamic polarization studies

The polarization curves of 43035SS in 2 M H_2SO_4/0% NaCl, 2 M H_2SO_4/1% NaCl, 2 M H_2SO_4/3.5% NaCl and 2 M H_2SO_4/6% NaCl at 308 K, 328 K, 348 K and 378 K are shown in Fig. 1(a)–(d). Table 2 shows the results of the curves. The corrosion rate in acid chloride solutions increases exponentially with increase in temperature, due to decrease in hydrogen evolution overpotential with increase in temperature [17]. The polarization curves at 308 K, 328 K, 348 K and 378 K in Fig. 1(a) shows the effect of changes in solution temperature on the corrosion and passivation characteristics of 43035SS without NaCl addition. Metastable pitting condition was completely absent from the polarization curves until 378 K due to the absence of Cl^- ions which tends to interfere with the passivation mechanism. Anodic passivity of metals results from the formation of Cr_2O_3. In general, the formation of passive film may occur according to solid state reaction mechanism in the following equations [18–21].

Please cite this article in press as: Loto RT, Loto CA. Corrosion behaviour of S43035 ferritic stainless steel in hot sulphate/chloride solution. J Mater Res Technol. 2017. http://dx.doi.org/10.1016/j.jmrt.2017.07.004

Table 1 – Percentage nominal composition of 43035SS.

Element symbol	Si	N	Ni	Mo	Ti	Cr	Mn	P	S	C	Fe
% Composition (43035SS)	0.75	0.03	0.2	0.1	0.335	17.35	0.50	0.04	0.03	0.01	80.655

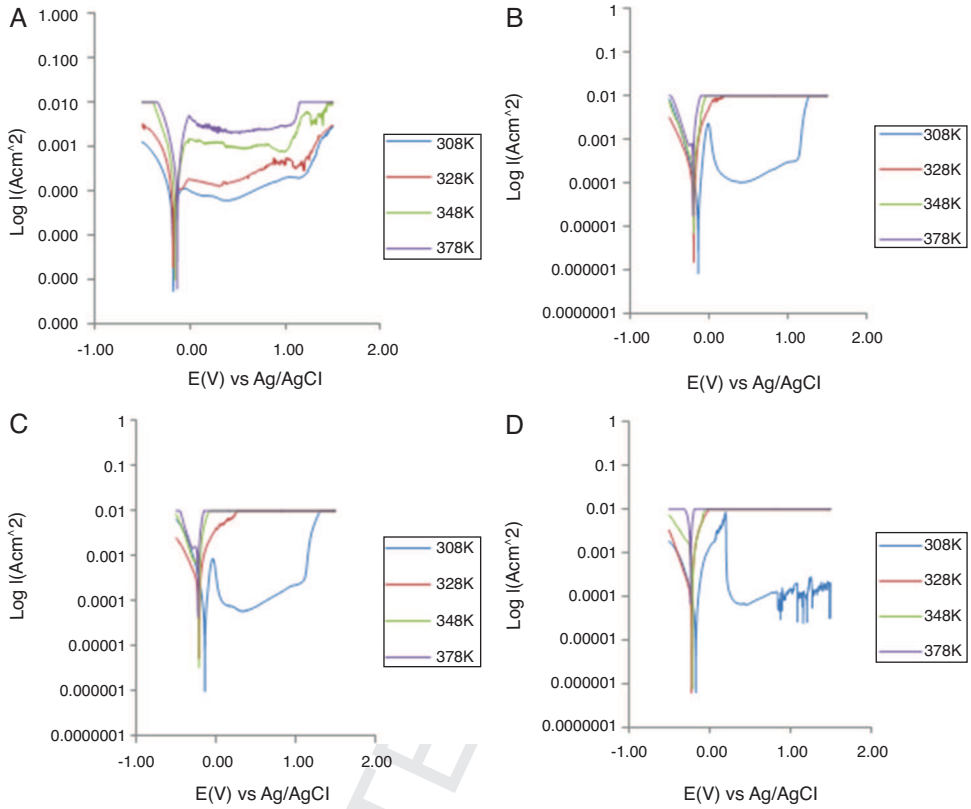

Fig. 1 – Potentiodynamic polarization curves of 43035SS in 2 M H_2SO_4 at (a) 0% NaCl, (b) 1% NaCl, (c) 3.5% NaCl and (d) 6% NaCl.

$$nM + mH_2O \rightarrow M_nOm + 2mH^+ + 2me^- \quad (1)$$

or precipitation reaction,

$$M^{2+} + nH_2O \rightarrow M(OH)_2(n-2)H_2O + 2H^+ \quad (2)$$

At 378 K, the increased mobility and electrolytic action of SO_4^{2-} ions slightly delayed the formation of the passive film on 43035SS resulting in metastable pitting activity. Increase in temperature generally hinders the interfacial reaction of chromium and oxygen, delaying the formation of the passive protective film which blocks ion-transfer processes associated with metal dissolution [22]. Cr_2O_3 is oxidized to CrO_2 and the protective Cr_2O_3 in the passive film is removed in stainless steels polarized above the transpassive potential in chloride free solutions [23,24]. The strength of the film was slightly influenced as shown on the passivation range at the temperatures studied, as a result temperature change has limited influence on the pitting potential, hence the pitting corrosion resistance of the steel. The results on Table 2 (2 M H_2SO_4/0% NaCl) for the polarization curve show a marginal but proportionate increase in corrosion rate and decrease in polarization resistance with respect to increase in temperature.

Studying the polarization curves in Fig. 1(b)–(c), 43035SS retains its passivity at ambient temperature of 308 K; however metastable pitting becomes more visible with increase in Cl^- ion (1%, 3.5% and 6%) concentration which delays the formation of stable passive film. Generally similar electrochemical behaviour was observed for 43035SS at 348 K and 378 K (Fig. 1(b) and (c), the corrosion rates for these figures are proportional to solution concentration and temperature (Table 2). The cathodic polarization curve of Fig. 1(b) and (c) at 378 K shows unusual activity signifying an increase in cathodic reaction rate probably due to major decrease in hydrogen evolution overpotential [25]. At Fig. 1(d), there is a significant increase in the metastable pitting region of curve at 308 K probably due to the significant concentration of Cl^- ion present (6% NaCl). Current transients and spikes are visible on the curve due to passivation and repassivation of the passive film before instantaneous failure of the steel. They signify pit initiation and propagation on the polarization curve due to loss of transpassivity as a result of irreversible collapse of the

Please cite this article in press as: Loto RT, Loto CA. Corrosion behaviour of S43035 ferritic stainless steel in hot sulphate/chloride solution. J Mater Res Technol. 2017. http://dx.doi.org/10.1016/j.jmrt.2017.07.004

Q7 **Table 2 – Potentiodynamic polarization results for 43035SS in 2 M H2SO4/0–6% NaCl concentration at 308 K, 328 K, 348 K and 378 K.**

Sample	Temp. (K)	Corrosion rate (mm/y)	Corrosion current (A)	Corrosion current density (A/cm^2)	Corrosion potential (V)	Polarization resistance, R_p (Ω)	Cathodic Tafel slope, B_c (V/dec)	Anodic Tafel slope, B_a (V/dec)
2 M H_2SO_4/0% NaCl								
A	308	0.39	4.60E−05	3.65E−05	−0.173	558.20	−7.223	3.169
B	328	0.92	1.08E−04	8.60E−05	−0.176	243.90	−7.547	1.261
C	348	1.25	1.47E−04	1.16E−04	−0.151	175.20	−10.690	10.820
D	378	2.57	3.02E−04	2.39E−04	−0.131	85.19	−10.160	9.852
2 M H_2SO_4/1% NaCl								
A	308	0.46	5.40E−05	4.29E−05	−0.133	475.80	−8.354	15.61
B	328	1.07	1.25E−04	9.92E−05	−0.189	205.60	−6.481	8.56
C	348	4.35	5.11E−04	4.05E−04	−0.189	50.31	−5.187	13.910
D	378	17.27	2.03E−03	1.61E−03	−0.197	12.69	−4.721	7.242
2 M H_2SO_4/3.5% NaCl								
A	308	0.70	8.25E−05	6.55E−05	−0.138	311.40	−8.638	9.815
B	328	2.72	3.19E−04	2.53E−04	−0.214	80.44	−4.175	6.264
C	348	11.95	1.40E−03	1.11E−03	−0.209	18.34	−2.861	6.534
D	378	21.21	2.49E−03	1.97E−03	−0.224	10.33	−2.380	2.980
2 M H_2SO_4/6% NaCl								
A	308	0.94	1.10E−04	8.72E−05	−0.168	491.40	−8.030	10.05
B	328	2.48	2.91E−04	2.31E−04	−0.221	88.25	−5.380	7.19
C	348	13.82	1.62E−03	1.29E−03	−0.211	67.42	−5.758	7.940
D	378	46.37	5.44E−03	4.32E−03	−0.232	4.73	−1.562	0.000

passive film [26,27]. At temperatures above 308 K [Fig. 1(b)–(d)], passivation behaviour was completely absent and the steel in effect polarized in the acid chloride solution similar to carbon steels [28]. 43035SS tends to more easily form soft acid from the concept Lewis acid–base theory at high temperature when compared to its behaviour at 308 K ambient temperature due to the increased oxidizing strength and mobility of the corrosive ions. Under this condition excessive adsorption of sulphates and chlorides ions accelerates the corrosion rate of the steel [29].

The corrosion potential, cathodic, and anodic Tafel slope values in Table 2 varies with respect to temperature and Cl^- ion concentration. The corrosion potential shifts positively with increase in temperature at 0% NaCl while the cathodic and anodic Tafel slope increases in value. At 1%, 3.5% and 6% NaCl the corrosion potential shifts to negative potentials consistent with visible increase in corrosion rate as the temperature rises while the cathodic and anodic Tafel slopes decreases. Variation in Cl^- ion concentration is responsible for these observations. In the absence of chlorides the increase in corrosion rate was marginal while the corrosion potential decreased due to strong resistance of the steel to anodic dissolution [30]. This shows that 43035SS is highly resistant to corrosion in the absence of chlorides even at the temperatures studied, retaining its passivation despite the increase in cathodic and anodic activity. However chlorides play a major role in the dissolution of stainless steels. In the presence of chlorides there was a significant increase in corrosion rate with respect to temperature but an unusual decrease in cathodic and anodic currents due to the metallurgical characteristics of the steel coupled with its corrosion resistance properties.

3.2. *Effect of temperature*

The relationship between the corrosion rate of 43035SS in the acid chloride solution and temperature is expressed by the Arrhenius equation which calculates the activation energy (E_a) of the steel corrosion using Arrhenius theory. Assumptions of Arrhenius theory is expressed by the following equation [31];

$$C_R = A \exp\left[\frac{E_a}{RT}\right] \quad (3)$$

where C_R is the corrosion rate, T the absolute temperature, R is the universal gas constant and A is the Arrhenius pre-exponential factor. The activation energy is the minimum amount of energy required for the H_2SO_4/NaCl solution to react with 43035SS surface. Plots of the logarithm of corrosion rate vs. 1000/T are given in Fig. 2. The plots obtained are straight lines and the slope of each straight line gives its activation energy E_a while the intercept give the Arrhenius pre-exponential factor.

The enthalpy and entropy of activation can be evaluated using the Transition state equation below [32].

$$C_R = \frac{RT}{Nh} \exp\left[\frac{\Delta S}{R}\right] \exp\left[-\frac{\Delta H}{RT}\right] \quad (4)$$

where h is Plank's constant, N is the Avogadro number, ΔS is the entropy of activation and ΔH is the enthalpy of activation.

Please cite this article in press as: Loto RT, Loto CA. Corrosion behaviour of S43035 ferritic stainless steel in hot sulphate/chloride solution. J Mater Res Technol. 2017. http://dx.doi.org/10.1016/j.jmrt.2017.07.004

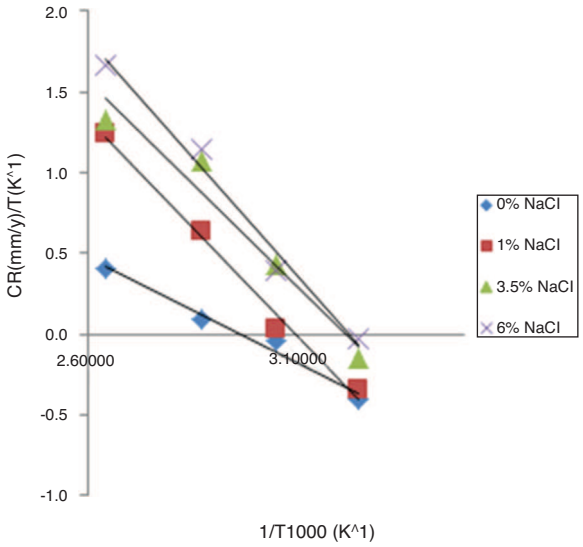

Fig. 2 – Arrhenius plots of Log C_R vs 1/T.

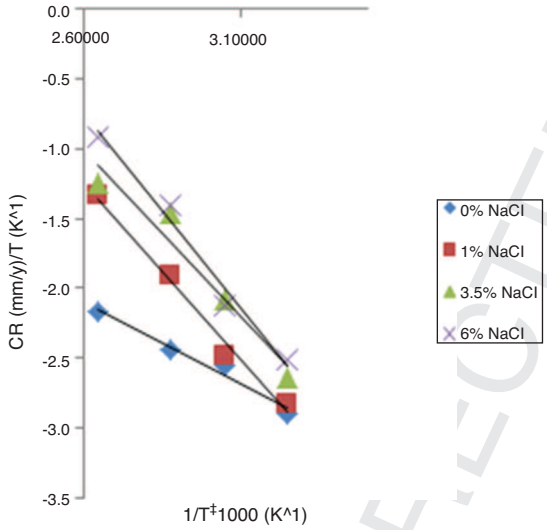

Fig. 3 – Transition state plot for Log C_R/T vs 1/T.

Plot of Log(C_R/T) vs 1/T (Fig. 3) where straight lines obtained with slope of ($\Delta H/R$) and an intercept of Log(R/Nh) + ($\Delta S/R$) from which the values of ΔH and ΔS were calculated.

Gibbs free energy was calculated from the relationship below [33];

$$\Delta G = \Delta H - T\,\Delta S \quad (5)$$

Results of enthalpy of activation, entropy of activation, activation energy and pre-exponential factor at different NaCl concentrations are shown in Table 3. The positive value of ΔS in Table 3 implies that the activation complex represents a disordering taking place from reactants to the activated complex. The degree of disorderliness continued to increase with increase in value of ΔS corresponding to increase in Cl^- ion concentration. The negative sign of the enthalpy (ΔH) at 0% NaCl concentration implies an exothermic nature of the steel corrosion reaction in the acid media at 308 K, 328 K, 348 K and 378 K involving the release of heat and low temperature dependence [34–37]. At 1%, 3.5% and 6% NaCl concentration the steel corrosion is endothermic as the chemical reaction involving chlorides absorbs energy coupled with increase in temperature [38–41]. The values of E_a decreases with increase in Cl^- ions signifying a decrease in passivation of the alloy surface due to accelerated dissolution process which consequently increases the corrosion rate [34]. This also shows that the energy barrier of the corrosion reaction decreases as the Cl^- ion concentration increases and transition state complex forms at a slower rate.

The change in ΔG for the corrosion reaction shows the reaction occurred spontaneously. The spontaneity of the reaction increased with addition of chlorides to the acid solution before the reaction shifts to equilibrium from the standard-state condition. The significant difference in the values of the activation parameters (E_a, ΔH, ΔS and ΔG) between the 0% NaCl steel samples and samples with variable Cl^- ion concentration indicates that there were essential changes in the dissolution mechanism of the steel in the presence and absence of chlorides [42].

3.3. *Statistical analysis*

Statistical analysis through ANOVA at a confidence level of 95% and 97.5% (significance level of $\alpha = 0.05$ & 0.025) was employed to calculate the statistical influence of Cl^- ion concentration and temperature on the corrosion rate value of 43035SS according to Eqs. (6)–(8).

The sum of squares among columns (temperature)

$$SS_c = \frac{\Sigma r_c^r}{nr} - \frac{r^2}{N} \quad (6)$$

Sum of squares among rows (NaCl concentration)

$$SS_r = \frac{\Sigma \tau_r^2}{nc} - \frac{\tau^2}{N} \quad (7)$$

Total sum of squares

$$SS_{Total} = \sum x^2 - \frac{\tau^2}{N} \quad (8)$$

Results in Table 4 showed that only temperature is statistically relevant, thus majorly responsible for the corrosion rate values of 43035SS with F-values of 5.256. This value is greater than the control significance factor (significance F) value of 5.078and 3.863 at 50.8%, confirming its relevance at the level of probability used. The results show that temperature variation strongly influences the corrosion behaviour and passivation characteristics of the steel in contrast to NaCl concentration which has a significant factor of 2.099 at 20.3%.

Please cite this article in press as: Loto RT, Loto CA. Corrosion behaviour of S43035 ferritic stainless steel in hot sulphate/chloride solution. J Mater Res Technol. 2017. http://dx.doi.org/10.1016/j.jmrt.2017.07.004

Table 3 – Results of enthalpy of activation, entropy of activation, activation energy and pre-exponetial factor at different NaCl concentrations.

NaCl concentration (%)	Arrhenius equation			Transition state equation			Gibbs free energy, ΔG (kJ/mol)
	Activation energy, E_a (kJ/mol)	Arrhenius pre-exponential factor, A (day^{-1})	Correlation coefficient, R^2	Enthalpy of activation, ΔH (kJ/mol)	Entropy of activation, ΔS (kJ/mol)	Correlation coefficient, R^2	
0	−1.31	3.88	0.9777	−1.16	0.91	0.9711	−281.44
1	−2.69	8.34	0.9885	2.54	5.38	0.9873	−1762.10
3.5	−2.54	8.17	0.9521	2.39	5.20	0.9456	−1807.21
6	−2.93	9.45	0.9829	2.78	6.48	0.9811	−2446.78

Table 4 – Analysis of variance (ANOVA) for 43035SS in 2 M H_2SO_4/0–6% NaCl (at 97.5% and 95% confidence level).

Source of variation	Source of variation	Sum of squares	Degree of freedom	Mean square	Mean square ratio (*F*)	Min. MSR at 97.5% confidence Significance *F*	Min. MSR at 95% confidence Significance *F*	*F* (%)
Among columns	NaCl Conc. (columns)	455.03	3	151.68	2.099	5.078	3.863	20.3
Among rows	Temperature (rows)	1139.33	3	379.78	5.256	5.078	3.863	50.8
Residual	Residual	650.33	9	72.26				
Total	Total	2244.69	15					

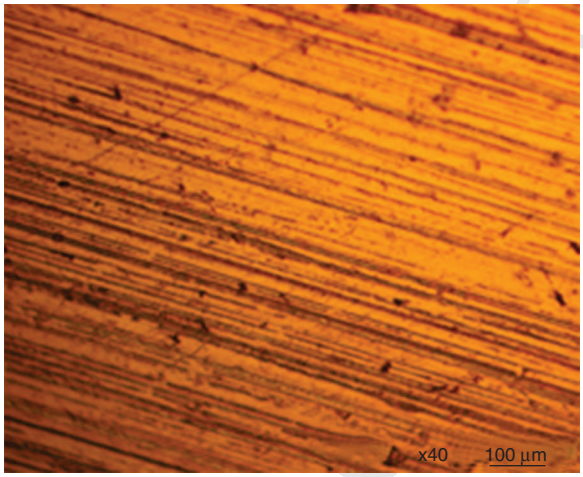

Fig. 4 – Optical image of 43035SS before corrosion test at mag. 40×.

3.4. *Optical microscopy analysis*

The optical images of 43035SS at 308 K and 378 K, before and after corrosion at specific Cl^- ion concentration are shown from Figs. 4–6(b). Fig. 4 shows the image of the steel sample before corrosion test at mag. 40×. Fig. 5(a) and (b) shows images of the steel sample after corrosion (mag. 40×) in 0% NaCl at 308 K and 378 K, while Figs. 7(a) and (b) shows the Q3 images of the steel sample after corrosion (mag. 40×) in 6% NaCl at 308 K and 378 K. The images in Fig. 5(a) slightly contrast the image in Fig. 4 due to mild surface deterioration whereby the lined serrated edges in Fig. 4 due to machining are worn out. The corrosion rate results (Table 2) for Fig. 5(a) sample was marginal, in effect Fig. 5(a) is an etched image of Fig. 4. The presence of SO_4^{2-} ions only in the corrosive test solution at ambient temperature of 308 K has limited effect on the corrosion resistance of 43035SS. At 378 K the visible surface deterioration are clearly shown with limited evidence of the presence of corrosion pits [Fig. 5(b)] due to the debilitating action of the SO_4^{2-} ions at high temperature. The deterioration is quite superficial damaging only the aesthetic value of the steel form observation of the corrosion rate results. The increase in corrosion rate from 308 K to 378 K for 43035SS at 0% NaCl is minimal. As such the value for E_a at 0% NaCl is the highest due to non-destruction of the passive protective film. Its ΔS, ΔH and ΔG are the lowest due to the exothermic nature of the reaction in the absence of chlorides, low spontaneity and disordering of the reaction process resulting in less damage to the steel morphology.

Studying the optical images in Fig. 7(a) and (b); the electrochemical action of Cl^- ions (6% NaCl) in 2 M H_2SO_4 solution is clearly visible on the surface morphology of 43035SS after corrosion test at 308 K and 378 K. Numerous corrosion pits have initiated and possibly propagating on the steel surface. The

Please cite this article in press as: Loto RT, Loto CA. Corrosion behaviour of S43035 ferritic stainless steel in hot sulphate/chloride solution. J Mater Res Technol. 2017. http://dx.doi.org/10.1016/j.jmrt.2017.07.004

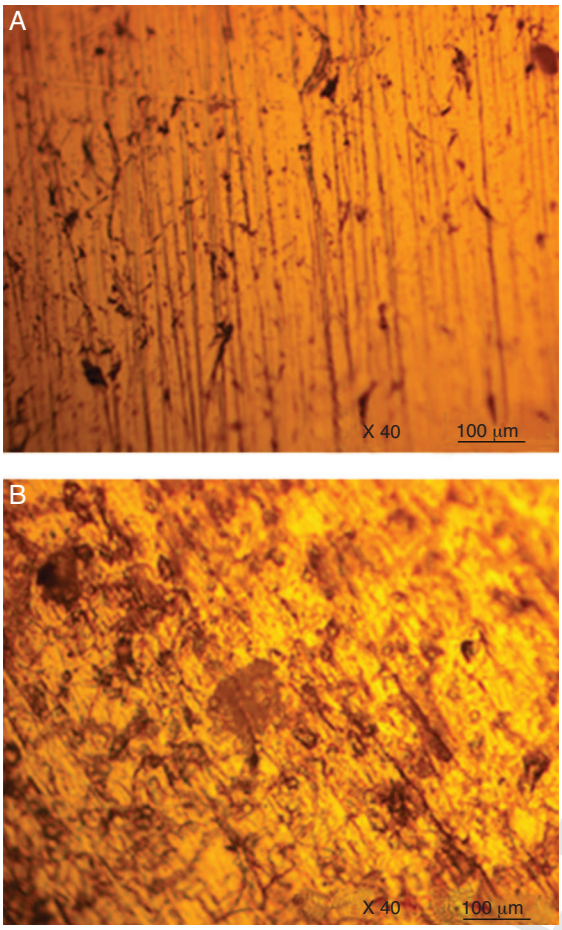

Fig. 5 – Optical image (mag. 40×) of 43035SS after corrosion in 0% NaCl (a) at 308 K, (b) at 378 K.

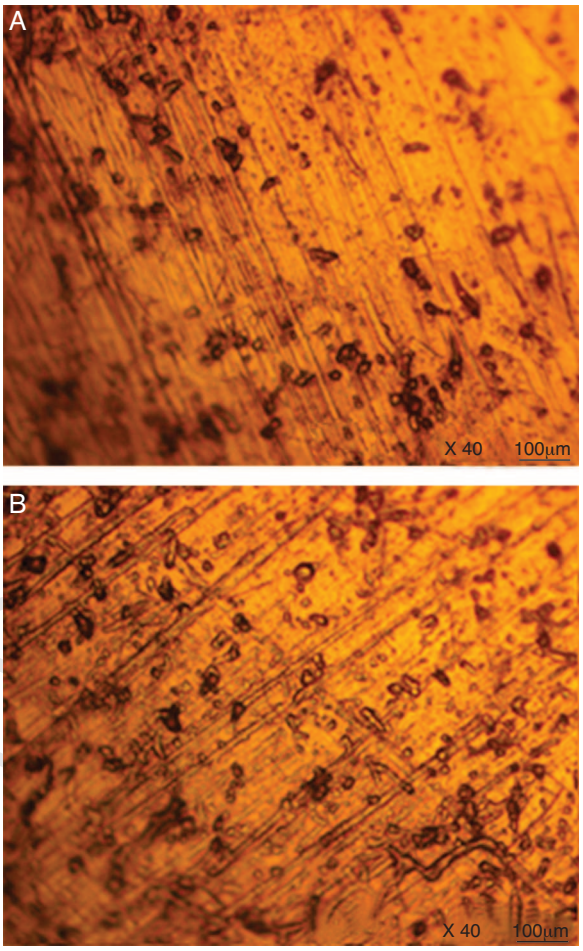

Fig. 6 – Optical image (mag. 40×) of 43035SS after corrosion in 6% NaCl (a) at 308 K, (b) at 378 K.

morphological difference between Fig. 7(a) and (b) is limited but the corrosion rate values of 0.94 mm/y and 46.37 mm/y varies widely. No visible surface deterioration were observed from eye observation except through optical microscopy, however optical microscopy analysis did not give anything unusual to explain the very high corrosion rate at 378 K. It is known that high alloy stainless steel do not undergo general corrosion but only corrode through pitting. It is suggested that the corrosion pits formed on 43035SS at 378 K are more advanced than the ones at 308 K. This assumption is confirmed from the very value of E_a (−2.93 kJ/mol) at this temperature and Cl^- ion concentration. The value signifies greater destruction of the passive film in comparison to the surface morphology of 43035SS at lower temperature and Cl^- ion concentration.

4. Conclusion

43035 ferritic stainless steel retained its passivity at temperatures of 308 K, 328 K, 348 K and 378 K in 0% NaCl, though the formation of its passive film delayed with increase in temperature. The presence of chlorides at specific NaCl significantly hindered the formation of the steels passive film at 308 K with the formation of metastable pits and decrease in the passivation range. At 6% NaCl the passive film failed at very low corrosion currents due to excess adsorption of chlorides. Temperature variation in the presence of chlorides significantly influenced the passivation behaviour of 43035 steel coupled with accelerated increase in corrosion rate. Optical microscopy analysis showed negligible surface deterioration of the steel at 378 K from 0% NaCl, however formation of corrosion pits were visible on samples at 308 K and 378 K from 6% NaCl. The steel corrosion reaction was exothermic in the absence of chlorides and endothermic with chloride addition. The entropy value increased while activation energy decreased with increase in NaCl concentration due to decrease in the passivation behaviour of the alloy. Statistical analysis through ANOVA at confidence levels of 95% and 97.5% showed the strong influence of temperature variation only on corrosion rate in contrast to the NaCl concentration whose value was below the significance level.

Conflicts of interest

The authors declare no conflicts of interest. Q4

Please cite this article in press as: Loto RT, Loto CA. Corrosion behaviour of S43035 ferritic stainless steel in hot sulphate/chloride solution. J Mater Res Technol. 2017. http://dx.doi.org/10.1016/j.jmrt.2017.07.004

Acknowledgement

The author acknowledges Covenant University Ota, Ogun State, Nigeria for the sponsorship and provision of facilities for the research project.

REFERENCES

[1] Abdallah M. Corrosion behaviour of 304 stainless steel in sulphuric acid solutions and its inhibition by some substituted pyrazolones. Mater Chem Phys 2003;82:786–92.
[2] Corrosion resistance of the austenitic chromium-nickel stainless steels in chemical environments. Available at http://www.parrinst.com/wp-content/uploads/downloads/2011/07/Parr_Stainless-Steels-Corrosion-Info.pdf.
[3] Bustein G, Rodriguez J, Romangoli R. Inhibition of steel corrosion by calcium benzoate adsorption in nitrate solutions. Corr Sci 2005;47:369–83.
[4] Tantawy N. Evaluation of new cationic surfactant as corrosion inhibitor for carbon steel in a metal working fluid. Ann Univ Dunărea JOS Galaţi Fascicle 2005;8:112–4.
[5] Beloglazov SM. Hydrogenation of steel in electrochemical processes. Leningrad: Publishing House of the Leningrad University; 1975.
[6] Stephen MM, Douglas D, Dunn JH. Metallurgical examination of cooling water equipment failures, Ashland Specialty Chemical Company, drew industrial. Analyst 2005.
[7] Wang K, Wang J, Hu W. Evaluation of temperature effect on the corrosion process of 304 stainless steel in high temperature water with electrochemical noise. Mater Design 2015;82:155–63.
[8] Guiñón-Pina V, Igual-Muñoz A, García-Antón J. Influence of temperature and applied potential on the electrochemical behaviour of nickel in LiBr solutions by means of electrochemical impedance spectroscopy. Corr Sci 2009;51(10):2406–15.
[9] Heusler KE. Growth and dissolution of passivating films. Corr Sci 1990;31:597–606.
[10] Reena KPD, Nayak J, Shetty AN. Corrosion behaviour of 6061/Al-15 vol. pct. SiC(p) composite and the base alloy in sodium hydroxide solution. Arabian J Chem 2012;9(2):S1144–54.
[11] Garverick L. Corrosion in the petrochemical industry. Materials Park, OH: ASM International; 1995.
[12] Outteridge T. Duplex stainless steel in pharmaceutical industry, p. 6. http://www.sswnews.com/pdf/Duplex_Stainless_Steel_in_Pharmaceutical_Industry.pdf.
[13] ASTM G59-97; 2014. Standard test method for conducting potentiodynamic polarization resistance measurements. Available at http://www.astm.org/Standards/G31.
[14] ASTM G1-03; 2011. Standard practice for preparing, cleaning, and evaluating corrosion test specimens. Available at http://www.astm.org/Standards/G1.
[15] ASTM G102-89; ~~2015~~. Standard practice for calculation of corrosion rates and related information from electrochemical measurements. Available at ~~http://www.astm.org/Standards/G31~~.
[16] Loto RT, Loto CA, Popoola API, Kupolati W. Corrosion inhibition effect of n, n′-diphenylthiourea on the electrochemical characteristics of mild steel in dilute acidic environments. J Chem Soc Pakistan 2016;38(2):222–33.
[17] Popova E, Sokolova E, Raicheva S, Christov MM. AC, and DC study of the temperature effect on mild steel corrosion in acid media in the presence of benzimidazole derivatives. Corr Sci 2003;45(1):33–58.
[18] Lorenz WJ, El Milgy D, Geana D. A theoretical treatment of the kinetics of iron dissolution and passivation. Electrochim Acta 1975;20(4):273–81.
[19] Lorbeer P, Lorenz WJ. The kinetics of iron dissolution and passivation depending on temperature and ionic strength. Corr Sci 1980;20(3):405–12.
[20] Poornima T, Jagannatha N, Shetty AN. Studies on corrosion of annealed and aged 18 Ni 250 grade maraging steel in sulphuric acid medium. Portugaliae Electrochim Acta 2010;28(3):173–88.
[21] Thomas PM, Hongjun Y, Fu-Ren FF, Allen JB. Electron-transfer reactions on passive chromium. J Electrochem Soc 1992;139(11):3158–67.
[22] Kruger J. In: Winstone RR, editor. Uhlig's corrosion handbook. John Wiley & Sons Inc.; 2011. p. 17.
[23] Bojinov M, Fabricius G, Laitinen T, Saario T. Transpassivity mechanism of iron–chromium–molybdenum alloys studied by AC impedance, DC resistance and RRDE measurements. Electrochim Acta 1999;44(21):4331–43.
[24] Larabi L, Harek Y, Benali O, Ghalem S. Hydrazide derivatives as corrosion inhibitors for mild steel in 1 M HCl. Prog Org Coat 2005;54(3):256–62.
[25] Landolt D. Passivity issues in tribocorrosion. In: 9th international symposium. 2006. p. 477–87.
[26] Riley AM, Wells DB, Williams DE. Initiation events for pitting corrosion of stainless steel? Corr Sci 1991;32(12):1307–13.
[27] Subir P, Anjan P, Sujit KG. Corrosion behavior of carbon steel in synthetically produced oil field seawater. Int J Metals 2014:628505, http://dx.doi.org/10.1155/2014/628505.
[28] Jensen WB. The Lewis acid–base concepts. New York: John Wiley & Sons, Inc.; 1980. p. 112–336.
[29] Muralidharan VS, Rajagopalan KS. Kinetics and mechanism of corrosion of iron in phosphoric acid. Corr Sci 1979;19(3):199–203, 205–07.
[30] Bouklah M, Hammouti B, Aounti A, Benhadda T. Thiophene derivatives as effective inhibitors for the corrosion of steel in 0.5 M H_2SO_4. Prog Org Coat 2004;49(3):225–8.
[31] Abd Ei-Rehim SS, Ibrahim MAM, Khaled KF. 4-Aminoantipyrine as an inhibitor of mild steel corrosion in HCl solution. J Appl Electrochem 1999;29(5):593–9.
[32] Goudarzi N, Farahani H. Investigation on 2-mercaptobenzothiazole behavior as corrosion inhibitor for 316-stainless steel in acidic media. Anti-Corr Methods Mater 2013;61(1):20–6.
[33] Atkins PW. Physical chemistry. 6th ed. Oxford University Press; 2000.
[34] Laidler KJ, Meiser JH. Physical chemistry. 3rd ed. Boston, USA: Houghton Mifflin Company; 1999.
[35] Anees AK, Aprael SY, Abdul AHK, Ahmed SA, Ahmed YM. The effect of temperature and acid concentration on corrosion of low carbon steel in hydrochloric acid media. Am J Appl Sci 2009;6(7):1403–9.
[36] Slemnik M. Activation energies ratio as corrosion indicator for different heat treated stainless steels. Mater Design 2016;89(5):795–801.
[37] Guiñón-Pina V, Igual-Muñoz A, García-Antón J. Influence of temperature and applied potential on the electrochemical behaviour of nickel in LiBr solutions by means of electrochemical impedance spectroscopy. Corr Sci 2009;51(10):2406–15.
[38] Gomma GK, Wahdan MH. Schiff bases as corrosion inhibitors for aluminium in hydrochloric acid solution. Mater Chem Phys 1995;39(3):209–13.

Please cite this article in press as: Loto RT, Loto CA. Corrosion behaviour of S43035 ferritic stainless steel in hot sulphate/chloride solution. J Mater Res Technol. 2017. http://dx.doi.org/10.1016/j.jmrt.2017.07.004

[39] Abdel-Gaber AM, Abd-El-Nabey BA, Sidahmed IM, El-Zayady AM, Saadawy M. Kinetics and thermodynamics of aluminium dissolution in 1.0 M sulphuric acid containing chloride ions. Mater Chem Phys 2006;98(2–3):291–7.
[40] Fontana MG, Green ND. Corrosion engineering. 2nd ed. New York: McGraw-Hill; 1978.
[41] Marsh J. Advanced organic chemistry. 3rd ed. New Delhi: Wiley Eastern; 1988.
[42] Blasco-Tamarit E, García-García DM, García-Antón J. Imposed potential measurements to evaluate the pitting corrosion resistance and the galvanic behaviour of highly alloyed austenitic stainless steel and its weldment in a LiBr solution at temperatures up to 150 °C. Corr Sci 2011;53(2):784–95.

Please cite this article in press as: Loto RT, Loto CA. Corrosion behaviour of S43035 ferritic stainless steel in hot sulphate/chloride solution. J Mater Res Technol. 2017. http://dx.doi.org/10.1016/j.jmrt.2017.07.004